**Atmospheric
Chemistry
and Physics**

Multi-species inversion of CH_4, CO and H_2 emissions from surface measurements

I. Pison, P. Bousquet, F. Chevallier, S. Szopa, and D. Hauglustaine

Laboratoire des Sciences du Climat et de l'Environnement, UMR1572, CEA-CNRS-UVSQ, IPSL, Gif-sur-Yvette, France

Abstract. In order to study the spatial and temporal variations of the emissions of greenhouse gases and of their precursors, we developed a data assimilation system and applied it to infer emissions of CH_4, CO and H_2 for one year. It is based on an atmospheric chemical transport model and on a simplified scheme for the oxidation chain of hydrocarbons, including methane, formaldehyde, carbon monoxide and molecular hydrogen together with methyl chloroform. The methodology is exposed and a first attempt at evaluating the inverted fluxes is made. Inversions of the emission fluxes of CO, CH_4 and H_2 and concentrations of HCHO and OH were performed for the year 2004, using surface concentration measurements of CO, CH_4, H_2 and CH_3CCl_3 as constraints. Independent data from ship and aircraft measurements and satellite retrievals are used to evaluate the results. The total emitted mass of CO is 30% higher after the inversion, due to increased fluxes by up to 35% in the Northern Hemisphere. The spatial distribution of emissions of CH_4 is modified by a decrease of fluxes in boreal areas up to 60%. The comparison between mono- and multi-species inversions shows that the results are close at a global scale but may significantly differ at a regional scale because of the interactions between the various tracers during the inversion.

1   Introduction

The impact of human activities on climate starts with the modification of the composition of the atmosphere. The increase in the concentrations of greenhouse gases and aerosols directly influences the radiative budget of the Earth system. Moreover, the interactions between these atmospheric compounds induce many indirect effects, with either positive or negative feedbacks on the climate. For instance, the carbon monoxide molecule (CO) does not impact atmospheric radiation much, but its concentration, through competition for hydroxyl radicals (OH), modulates that of methane (CH_4), which is the second anthropogenic greenhouse gas after carbon dioxide (CO_2). Taking these interactions into account is an essential issue for forecasting the climate, as for interpreting the variations of the atmospheric composition. For this purpose, observation and modeling are two essential and complementary tools. Since the end of the 1950s, the number of in situ measurements of atmospheric compounds has been increased several fold. Structured in networks, the stations now provide data of a very high degree of accuracy (usually less than 0.1% for methane for example (GLOBALVIEW-CH4, 2005)) but with sparse and heterogeneous spatial coverage. The observation by satellite gradually supplements this lacunar network, though with a weaker measuring accuracy (usually around 1% for methane with the UV/Vis/near infrared spectrometer SCIAMACHY (Frankenberg et al., 2005)). Since the end of the 1980s, the modeling of the bio-geochemical cycles has made it possible to better understand the life cycles of greenhouse gases. Further, following the example of weather forecasting, the assimilation of bio-geochemical data in chemical transport models (CTM) has allowed, during the last decade, to produce better estimates of the emissions of gases and aerosols up to the subcontinental scale (Bergamaschi et al., 2007; Bousquet et al., 2000, 2006; Pétron et al., 2004; Rayner et al., 1999; Dubovik et al., 2008). Up to now, gas emissions have been treated independently from each other: emissions of CH_4 (Bergamaschi et al., 2007; Bousquet et al., 2006), CO (Chevallier et al., 2009; Pétron et al., 2004), hydrogen (H_2) (Price et al., 2007) and OH variations (Bousquet et al., 2005; Krol et al., 2003; Prinn et al., 2005) have been optimized independently from one another, or coupled only partially (Butler et al., 2005), whereas they are linked through chemical reactions and transport. At the mesoscale, in the framework of

air quality, Elbern et al. (2007) have studied the feasibility of the inversion of emissions of sulphur dioxide and ozone precursors. At a global scale, Stavrakou and Müller (2006) have inverted CO emissions taking into account their relation to the non-methanic volatile organic compounds (NMVOCs) through OH. In this work, we describe an inversion system that optimizes the four main reactive species of the methane oxidation chain (CH$_4$, CO, formaldehyde (HCHO) and H$_2$) within one framework. OH concentrations are also optimized from methyl chloroform (MCF) measurements.

The variational system used for this study, based on the Bayesian theory, is described in Sect. 2: its principal components are the global circulation model LMDz (Sect. 2.2.1) associated with the simplified chemistry model SACS (Sect. 2.2.1). In this study, the emissions that are optimized through the inversion are CH$_4$, CO and H$_2$ fluxes at the resolution of the grid of the model (no spatial aggregation in big regions). MCF emissions are used to constrain the optimization of OH concentrations within the inverse system. After having exposed the methodology, we study the year 2004 and make a first attempt at evaluating the inverted fluxes is described. All the prior inventories used in the model are described in Sect. 2.3. The observations used as constraints are surface measurements of MCF, CH$_4$, CO and H$_2$ concentrations (Sect. 2.4). After an evaluation of the results of the forward simulation (Sect. 3.1), the results of the inversion and an estimate of error reductions are detailed in Sect. 3.2. We then compare our optimized emissions to results obtained with different methods, particularly with mono-species inversions with the same system (Sect. 3.3), and our optimized concentrations to independent satellite, ship and aircraft data (Sect. 3.4).

2 The variational inversion system

2.1 Inversion system

The system relies on Bayesian inference as described by Chevallier et al. (2005) to combine observations and model results in order to estimate sources and sinks of atmospheric compounds. In contrast to the studies carried out up to now for the estimation of gaseous emissions (such as for example Gurney et al. (2002),Peylin et al. (2005)), in this study, the inversion is formulated in a variational framework. The problem to be solved is the minimization of a cost function of a state vector **x**, in the same way as Chevallier et al. (2005). The state vector **x** contains:

- the emission fluxes for selected species (CO, CH$_4$ and MCF net fluxes (sources and sinks balance) plus H$_2$ fluxes) in all model's grid cells at the surface and at an 8-day frequency

- the average production of HCHO due to VOCs in all model's columns (i.e. over each surface grid cell) and at an 8-day frequency

- the average OH concentrations over the column for four bands of latitude, as described in Bousquet et al. (2005) and at an 8-day frequency

- the initial conditions of concentrations of all species (but OH radicals) in all model's grid cells at the beginning of the inversion time-window (one year in this study).

The inversion system finds the optimal **x**$_a$ that fits both the observations **y**, the error statistics of which are represented by the covariance matrix R, and the prior fluxes **x**$_b$, for which the covariance matrix B specify their error statistics. The cost function J to be minimized is then defined as:

$$J(\mathbf{x}) = \qquad\qquad\qquad\qquad\qquad\qquad (1)$$
$$(\mathbf{x} - \mathbf{x}_b)^T B^{-1}(\mathbf{x} - \mathbf{x}_b) + (H(\mathbf{x}) - \mathbf{y})^T R^{-1}(H(\mathbf{x}) - \mathbf{y})$$

where H is the operator representing the chemistry-transport model plus convolution operation which gives the equivalent of observations from variables **x**. Note that following the common usage, it is assumed that the error statistics of observations and prior information are unbiased and Gaussian. One of the advantages of the variational formulation is its larger flexibility to deal with non-linearities in the forward model, i.e. non quadraticity of the cost function J, which is important for chemistry. The minimization of J is performed with the algorithm M1QN3 (Gilbert and Lemaréchal, 1989). The inversion system is based on the one described by Chevallier et al. (2005) to estimate CO$_2$ emissions. For this study, a simplified version of the module of atmospheric chemistry INCA (INteraction Chemistry - Aerosols) of Institut Pierre-Simon Laplace (IPSL), called SACS (Simplified Atmospheric Chemistry Assimilation System) and detailed in Sect. 2.2.2, has been coupled to the atmospheric transport model LMDz (Laboratoire de Météorologie Dynamique - Zoom, see Sect. 2.2.1). The system is ready to use satellite, aircraft and mobile or fixed surface data for the inversion of the emissions of the four species on periods of several years. In this first study, surface data are used for the inversion of emissions during the year 2004 and satellite, ship and aircraft data are used for direct comparison.

2.2 Modeling tools

2.2.1 LMDz and its adjoint

The model used here is the off-line version (LMDzt) of the general circulation model of the Laboratoire de Météorologie Dynamique (LMDz) (Sadourny and Laval, 1984; Hourdin
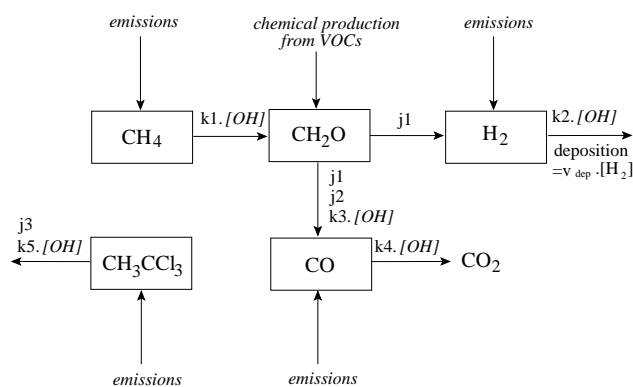
Fig. 1. Schematic of the simplified chemistry mechanism SACS: j1-3 and k1-5 are the constants of the reactions or of ensembles of reactions. [OH] and the variables indicated in italics are directly optimized by the data assimilation system.

and Armengaud, 1999). LMDzt is used here with nineteen sigma-pressure levels in the vertical (first level thickness of 150 m, resolution in the boundary layer of 300 to 500 m and ≈2 km at tropopause) and a horizontal resolution of $3.75° \times 2.5°$ (longitude-latitude). The air mass fluxes used off-line were pre-calculated by LMDz on-line GCM nudged on ECMWF analysis for horizontal winds. LMDz has been used for atmospheric studies for gases (Bousquet et al., 2005, 2006; Carouge et al., 2008a,b) and aerosols (Boucher et al., 2003) and climatological studies (IPCC, 2007).
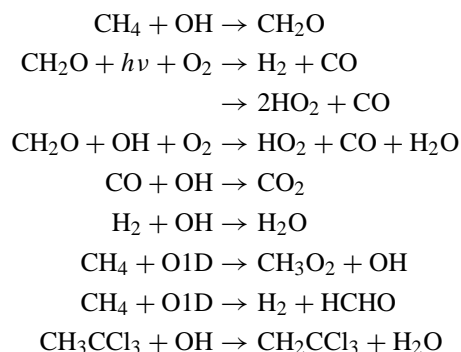
The tangent-linear and the matching adjoint codes of the transport of non-reactive gases in LMDz, including advection, convection and turbulence in the boundary layer have been described by Chevallier et al. (2005). The chemistry module (direct, tangent-linear and adjoint of SACS described below) has been developed for this work.

2.2.2 SACS

We decided to include a simplified chemistry module in this study, because i) of the lack of direct observations of many of the compounds used in the full INCA model, ii) of the computational burden of the inversion with a full chemistry model and iii) of the fact that it is possible to isolate a few principal reactions in the methane oxidation chain. This simplified chemistry module called SACS (Simplified Atmospheric Chemistry Assimilation System) is based on the INCA chemistry model (Hauglustaine et al., 2004; Folberth et al., 2005). It is a simplified forward and adjoint chemistry module for hydrocarbon and carbon monoxide degradation described in Fig. 1.

Methane is located upstream the chemical reaction chain considered here. The nature of its sources is well established (mainly anaerobic processes in wetlands, rice paddies, waste disposal sites, ruminant stomachs and termites and also fires,

production and consumption of gas and oil), even if their space-time variations are still poorly given at the regional scale (Bergamaschi et al., 2007; Bousquet et al., 2006). In the atmosphere, oxidation by OH is the main sink of CH$_4$ (its lifespan is then approximately 9 years (IPCC, 2007)). This reaction is the first in a chain of photochemical transformations which lead to formaldehyde (HCHO or CH$_2$O), also produced by the degradation of volatile organic compounds (VOCs) mainly in the continental boundary layer. In the atmosphere, within a few hours, HCHO is oxidized by OH and photolyzed to produce CO and H$_2$. CO is also emitted by the combustion of biomass and fossil fuels. Within a few months, CO is then oxidized by OH in carbon dioxide (CO$_2$). H$_2$ is also directly emitted by industries and the combustion of fossil fuels and taken out of the atmosphere by deposition on the land surface (probably under the action of enzymes) (Hauglustaine and Ehhalt, 2002). OH is the essential modulator of this reaction chain but this short-lived compound is not easily measurable. Its global concentration is observed only in an indirect way: using methyl chloroform (CH$_3$CCl$_3$ or MCF) which reacts only with OH and sources of which are quantified with a good accuracy (Krol et al., 2003; Prinn et al., 2005; Bousquet et al., 2005). One originality of this work is to include the constraints given by MCF concentration measurements directly within the inverse system.

The intermediate reactions not represented in Fig. 1 are considered as very fast compared to the reactions described in SACS as:

$$CH_4 + OH \rightarrow CH_2O$$
$$CH_2O + h\nu + O_2 \rightarrow H_2 + CO$$
$$\rightarrow 2HO_2 + CO$$
$$CH_2O + OH + O_2 \rightarrow HO_2 + CO + H_2O$$
$$CO + OH \rightarrow CO_2$$
$$H_2 + OH \rightarrow H_2O$$
$$CH_4 + O1D \rightarrow CH_3O_2 + OH$$
$$CH_4 + O1D \rightarrow H_2 + HCHO$$
$$CH_3CCl_3 + OH \rightarrow CH_2CCl_3 + H_2O$$

Note that products that are not indicated are not taken into account in the model. In addition, H$_2$ deposition is parameterized as: $H_{2\text{ deposited}} = v_{\text{dep}}.[H_2]$ where v_{dep} is the deposition velocity. Reaction kinetic and photolysis rates of SACS are those of LMDz-INCA (Folberth et al., 2006). OH concentrations, the three-dimensional chemical production of HCHO by VOCs and v_{dep} are taken from a full forward simulation by LMDz-INCA, as well as fields of species which are not tracers in SACS, such as O$_2$ or O1D. Photolysis of MCF was not taken into account for this one year inversion.

The adequacy of SACS has been evaluated against the full chemistry-transport model LMDz-INCA, as illustrated in Fig. 2: the same simulation (same meteorology, same initial
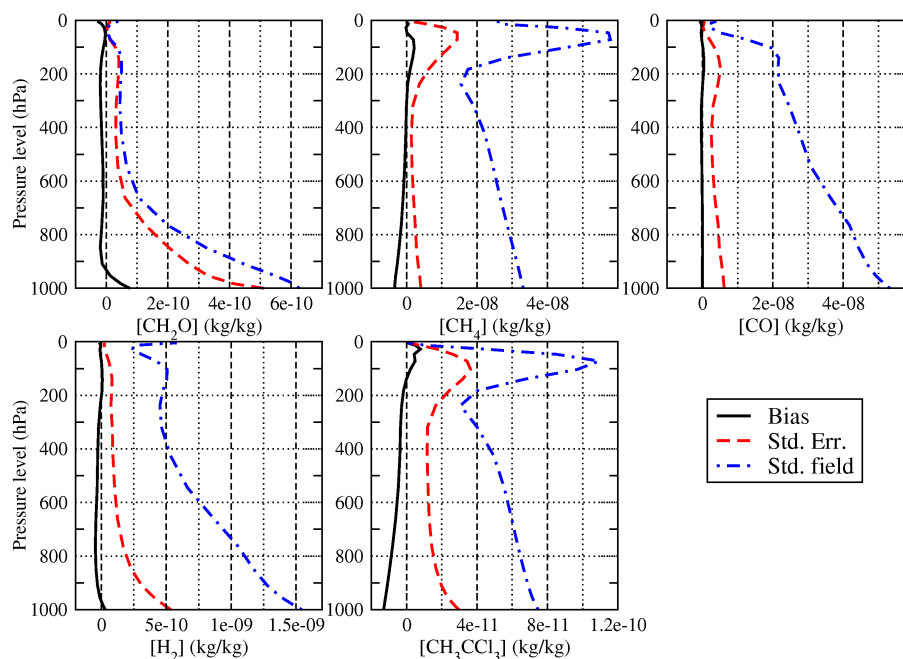
Fig. 2. Vertical profiles of bias and standard deviation (Std. Err.) of the differences between instantaneous concentrations (kg kg^{-1}) of formaldehyde (CH$_2$O, top left), methane (CH$_4$, top middle), carbon monoxide (CO, top right), hydrogen (H$_2$, bottom left) and methyl chloroform (CH$_3$CCl$_3$ = MCF, bottom middle) obtained with LMDz off-line plus the simplified chemistry mechanism SACS and LMDz on-line plus the full chemistry mechanism INCA after one-month simulations: example of January 2004. The field standard deviation (Std. field) profile corresponds to the field computed with INCA.

conditions, those of January 2004) has been performed with the full chemistry mechanism INCA and the simplified mechanism SACS. The vertical profile of the bias and of the standard error between the two sets of concentrations have then been computed for the five SACS tracers. The biases between the fields simulated with SACS and INCA are very small, with a maximum of 0.077 ppbv (parts per billion by volume) $(0.8 \times 10^{-10}$ kg kg$^{-1})$ for CH$_2$O, -5.4 ppbv $(-0.3 \times 10^{-8}$ kg kg$^{-1})$ for CH$_4$, -0.021 ppbv $(-0.2 \times 10^{-10}$ kg kg$^{-1})$ for CO, 0.43 ppbv $(0.3 \times 10^{-10}$ kg kg$^{-1})$ for H$_2$ and 0.003 ppbv $(1.3 \times 10^{-11}$ kg kg$^{-1})$ for MCF. The field standard deviation profile indicates that the variability of the whole field as computed with INCA is 1.2 (for CH$_2$O at the surface) to 26.4 (for H$_2$ at the top) times bigger than the difference between the two mechanisms as indicated by the standard deviation profile. This means that for each one of the five species, the differences between the two chemistry models are significantly smaller than the variability of the concentration field.

2.3 Emission inventory

Two main datasets are combined to build the prior inventory:

– the Emission Database for Global Atmospheric Re-

search (EDGAR v3) inventory for the year 1995 for anthropogenic emissions (Olivier and Berdowski, 2001)

– the Global Fire and Emission database (GFED-v2) (van der Werf et al., 2006) for monthly emissions due to biomass burning for the year 2004.

In addition, other sources are taken into account:

– emissions of CH$_4$ due to wetlands and termites based on the study by Fung et al. (1991)

– the biogenic emissions of H$_2$ based on Hauglustaine and Ehhalt (2002)

– an oceanic source of CO, equivalent to $\approx$20 Tg per year.

For MCF emissions, the inventory by Montzka et al. (2000) is rescaled according to an update of the study by Bousquet et al. (2006). Note that for the other species, no effort is made here to adapt the 1995 EDGAR 3 inventory to the year 2004. Since global economic growth occurred since 1995 and induced a modification of the emissions (Ohara et al., 2007), in particular in Asia, the results of the inversions performed here combine both the corrections on the bottom-up emissions and the trends over the 1995–2004 period.
The errors (variances, spatial and temporal correlations) of this prior information are modeled, based on physical considerations as detailed in Chevallier et al. (2005). In this study,
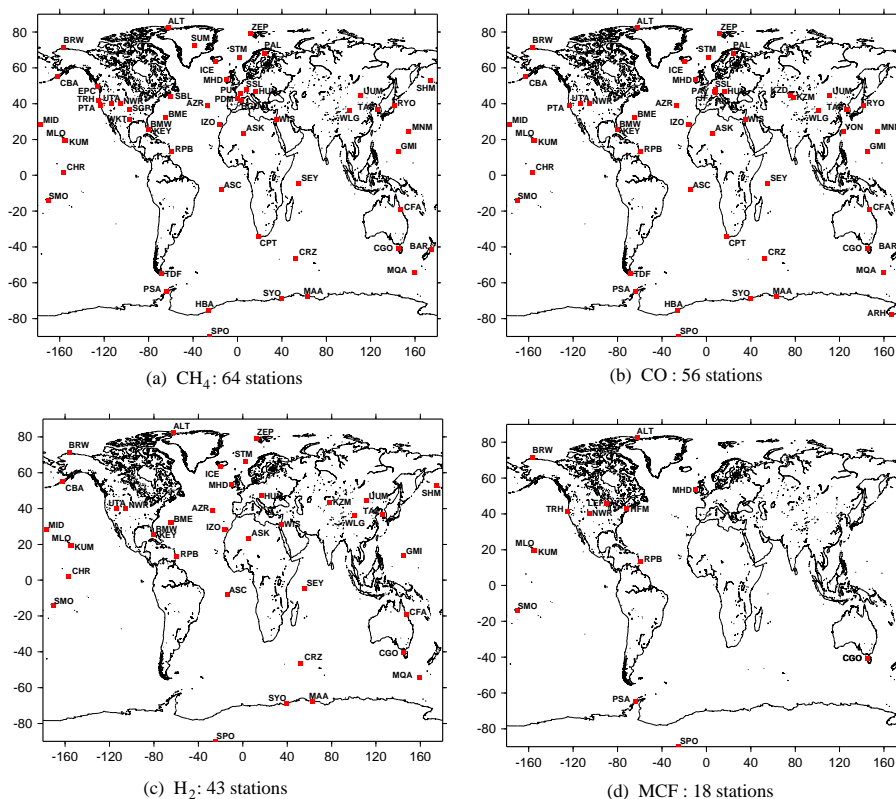
Fig. 3. Measurement surface stations for methane (top left), carbon monoxide (top right), hydrogen (bottom left) and methyl-chloroform (MCF, bottom right) used in our study over the year 2004.

the errors are then set to 100% of the maximal flux in the grid cell over the inversion period for CO and CH₄ (which allows for large analysis increments over the whole period), 100% of the flux for H₂, 1% of the flux for MCF (in order to constrain OH), 100% for HCHO concentrations, 10% for OH concentrations, 10% for the initial concentrations of HCHO and MCF and only 3% for CH₄ and 5% for CO. Temporal correlations are neglected. Correlation lengths of 500 km on land and 1000 km on sea are used (land and sea are not correlated). Through time, fluxes are defined over periods of eight days.

For 2004, the total emissions are 490 Tg of methane (including soil uptake), 1059 Tg of CO, 0.013 Tg of MCF and 39.3 Tg of H₂.

2.4 Atmospheric measurements

The observations used in this study are concentration measurements performed at surface stations for MCF (Montzka et al., 2000), CH₄ (Dlugokencky et al., 1994; Cunnold et al., 2002; Worthy et al., 1998), H₂ (Novelli et al., 1999) and CO (Novelli et al., 1992) from various networks (NOAA (Conway et al., 1994), CSIRO (Francey et al., 1999), AGAGE (Prinn et al., 2000), NIWA (Lowe et al., 1991), JMA/MRI

(Matsueda et al., 2004)) available on the World Data Centre for Greenhouse Gases (WDCGG) site at http://gaw.kishou. go.jp/wdcgg/. We used instantaneous measurements and data that are 24-h averages (named "event" and "daily" data in the database). Continuous measurements by the AGAGE network were averaged over 24 h and these daily means were used. We added observations available from the RAMCES (Réseau Atmosphérique de Mesure des Composés à Effet de Serre) network coordinated by LSCE (Schmidt et al., 2006). Among all the available stations, only those with enough measurements in 2004 (i.e. more than one value per month) were selected. The locations of the stations for the four tracers are displayed in Fig. 3.

For methane, all measurements were adjusted on the NOAA 2004 calibration scale (Dlugokencky et al., 2005) with the factors provided by GLOBALVIEW-CH4 (2005) and GLOBALVIEW-CO (2005).

The errors on observations were set as follow. For CO and CH₄, we used yearly means of synoptic variability from GLOBALVIEW; for MCF, we used yearly or monthly values from Prinn et al. (2005) or from the NOAA; and for H₂, data from CSIRO or from the NOAA were used. It is assumed here that the synoptic variability is an approximation of the transport errors, which is consistent with the weaknesses of

global models in reproducing continental synoptic concentrations of trace gases (Geels et al., 2007). Otherwise, if these data were not available, the uncertainties associated with the measurements were used. In all cases, a minimum uncertainty of ± 3 ppbv for CH_4, CO and H_2 and ± 1.2 ppt for MCF is fixed, in order to account for a minimal representativity error.

For the inversion, measurements are thinned so that only one measurement per grid cell per dynamical time step (30 min) is kept. Moreover, after comparison with the a priori forward simulation, measurements for which the matching simulated concentration is out of a range of 3σ were not used as constraints for the inversion. This finally leads to keep 169 to 225 constraints per month of the year 2004 for CO, 305 to 454 for CH_4, 127 to 193 for H_2 and 264 to 302 for MCF.

3 Results

3.1 A priori forward simulation

The year 2004 is simulated by the forward model LMDz-SACS. For methane and MCF, the initial conditions have been taken from the results obtained by Bousquet et al. (2006) for 2004; for the other tracers, the initial conditions are given by a simulation by LMDz-INCA as indicated in Sect. 2.2.2.

The performance of the a priori simulation is summarized by three statistical indicators displayed in Table 1: the bias, the standard deviation and the correlation between simulated concentrations and measurements at the stations. The weak correlation for H_2 is explained by a poor reproduction of the seasonal cycle that may be corrected by the inversion of emissions.

Table 2 shows the balance between sources (emissions and chemical production) and sinks (chemical loss and deposition): it verifies that CO and CH_4 do not accumulate much in the atmosphere but about 16.2 Tg of H_2 accumulate during the year. This unrealistic accumulation is partly due to a known underestimation of the deposition velocities (Hauglustaine and Ehhalt, 2002), particularly at high latitudes. A test with deposition velocities increased by 30% North of 60° of latitude shows that the accumulation of H_2 is only reduced to 15.4 Tg. Nevertheless, since no further information on deposition velocities was available at the time of this study, we chose to keep the field provided by LMDz-INCA and test the ability of the inverse system to deal with this problem.

Note that MCF emissions are very small since early 1995, after decades of large industrial use. The accumulated molecules are still being taken out of the atmosphere by chemical reaction with OH radicals. These conditions give a lifetime of about 2.6 months for CO. The values of lifetimes for CH_4, MCF and H_2 are not relevant since the for-

ward model is not completely at equilibrium after only one year of simulation.

3.2 Inversion

The emission fluxes of CO, CH_4, H_2 and MCF have been simultaneously inverted from January to December. After 20 iterations, the norm of the gradient of the cost function is reduced by about 83%. Due to the computational burden of the inversion with the chemical scheme, it was checked that the convergence was satisfying enough on emission fluxes (particularly CO and CH_4) for a first attempt at evaluating the inverted fluxes.

Concentrations

To assess the overall impact of the optimized emissions on concentrations, first-guess and analyzed scatter-plots with simulated concentrations as function of the measurements over the whole year for all stations for each species are displayed in Fig. 4.

The fit between simulated and observed CH_4 concentrations, which is already quite good for the first-guess (slope = 0.98), remains almost the same after inversion with a slope of 0.97 for a correlation coefficient of 0.97.

For CO concentrations, the underestimation of ≈24% by the model is reduced to ≈6% after inversion (slopes of 0.76 and 0.94).

As shown by the shapes and correlation coefficients for H_2 scatter-plots, the inversion only partially improves the poor fit between simulation and observations: both slopes and both correlation coefficients are still less than 0.6. Indeed, this poor fit of simulated concentrations is not caused exclusively by the emission inventory (see Sect. 3.1). The inversion corrects what can be modified by changing the emissions. Because the prior inventory and the model (chemistry and transport) have a weight in the optimization, the inversion cannot propose totally unrealistic fluxes to match the constraints on concentrations. More work is needed on the input data and on the chemistry of H_2.

The scatter-plot for MCF clearly shows that after inversion the concentrations are better adjusted to OH. The small groups of points that lay outside the main clouds are an artefact of a change at one station (NWR) during the year. Since prior concentrations for OH simply come from LMDz-INCA interactive simulation, prior MCF and OH are not precisely in equilibrium. The inversion of emissions, OH concentrations and initial conditions is able to correct this.

The same statistical indicators as for the forward simulation are computed for the optimized emissions, as displayed in Table 1. For CO and CH_4, the median biases are largely decreased (by more than 85%) and the correlations, which were already quite good are only slightly increased after the inversion (less than +5%). The median standard deviation is slightly increased for CO but significantly decreased (by

Table 1. Median values over all the stations for bias, standard deviation and correlation coefficient between simulated and measured concentrations in 2004: before inversion (in plain font), **after inversion** (in bold) and *difference* between posterior and prior absolute values in % of the prior absolute value (in italics).

Species	bias (ppbv)		standard deviation (ppbv)		correlation	
	prior	analysis	prior	analysis	prior	analysis
MCF	$9.8.10^{-4}$	$\mathbf{-4.1.10^{-4}}$	$4.6.10^{-4}$	$\mathbf{4.2.10^{-4}}$	0.96	**0.96**
CO	10.7	**−0.6**	9.1	**9.6**	0.86	**0.90**
		−94%		*+5.5%*		*+4.6%*
CH_4	−0.8	**−0.1**	11.3	**9.6**	0.81	**0.82**
		−87%		*−15.%*		*+1.2%*
H_2	−0.9	**1.8**	15.9	**13.8**	0.22	**0.37**
		+100%		*−13.2%*		*+68.2%*

Table 2. Mass balances in Tg for the year 2004: before inversion (in plain font), **after inversion** (in bold) and *difference in %* of the prior value between after and before inversion (in italics). Burden = average burden in the troposphere (up to level 12 of the model) over the year. Accumulation = (emission+production)-(loss+deposition).

Species	emissions		chemical production		chemical loss		deposition		burden		accumulation	
MCF	0.013106	**0.013106**	—		0.081625	**0.084252**	—		0.399223	**0.427202**	−0.068	**−0.071**
CO	1058.6	**1413.0**	1212.2	**1179.3**	2284.0	**2578.3**	—		337.3	**373.1**	−13.2	**14.0**
		+33.5%		*−2.7%*		*+12.9%*				*+10.6%*		*+202.9%*
CH_4	490.4	**491.5**	—		504.0	**488.7**	-		4334.2	**4343.5**	−13.6	**2.8**
		+0.2%				*−3.%*				*+0.2%*		*+120.6%*
H_2	39.3	**36.2**	39.3	**38.6**	18.6	**17.9**	43.8	**43.5**	167.6	**165.4**	16.2	**13.4**
		−7.9%		*−1.8%*		*−3.8%*		*−0.7%*		*−1.3%*		*−17.3%*

15%) for CH_4. For H_2, the median bias, which was small for the first-guess, is increased but remains below 2 ppbv, i.e. less than 0.5% of the global average measured concentration; the median standard deviation is significantly decreased (by more than 13%) and the correlation, which is low and denotes a poor seasonalization (see Sect. 3.1), is increased by almost 70%.

Mass budgets

The balance between sources and sinks with optimized emissions is displayed in Table 2. A small accumulation of 14.0 Tg of CO (less than 1% of the emitted mass) and of 2.8 Tg of CH_4 (less than 0.6% of the total emissions) is caused by the inversion for the year 2004. H_2 still accumulates during the year after the inversion: the non-linearity of the problem explains why the inverse system cannot totally correct the already poor first-guess. Nevertheless, the accumulated mass of H_2 in 2004 is decreased by 17.3% down to 13.4 Tg, principally through the decrease of emissions by almost 8%. More work is needed to fully understand the behavior of H_2 in the process.

For CH_4, these results might be compared to two previous studies. Bergamaschi et al. (2007) inverted CH_4 emissions for 2003 with the TM5 model, various prior inventories and either SCIAMACHY satellite or NOAA ESRL surface measurements. With a fixed total prior emitted mass at 507.7 Tg of CH_4, their analysis for 2003 ranges from 508.8 to 554.4 Tg. In the same framework, Meirink et al. (2008) compared synthesis and 4-D-var inversions. With the total prior emitted mass at 507.7 Tg, their analysis ranges from 523.5 to 525.2 Tg. With a prior for 2004 of only 490.4 Tg, our analysis at 491.5 Tg is on the lower side of this range. For CO, the study of Pétron et al. (2004) inverted emissions with a sequential scheme and MOPITT satellite data from April 2000 to March 2001. From a prior total emitted mass of 1034 Tg, their inversion ranges from 1228 to 1384 Tg. Our analysis of 1413.0 Tg for 2004 is higher but the large interannual variability of wildfires must be taken into account.

Emissions

CO The gradient between the two hemispheres, computed from the median values at the stations in each hemisphere,
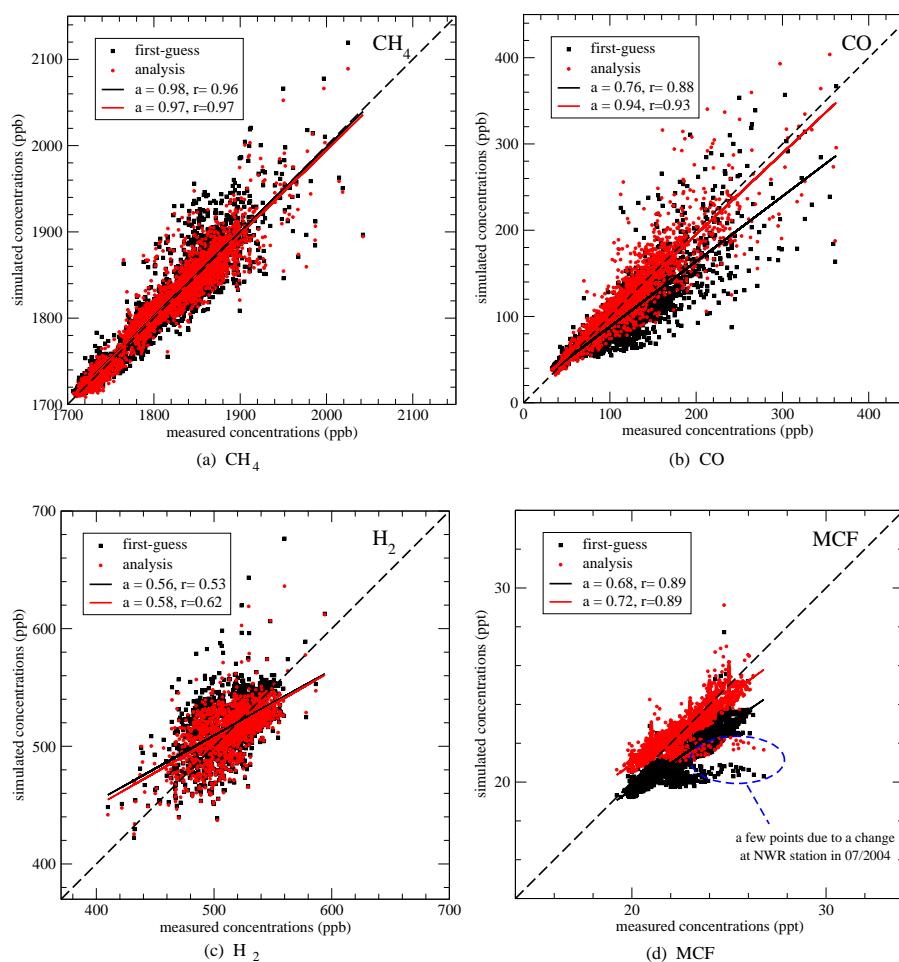
Fig. 4. Simulated first-guess and analyzed concentrations compared with measurements at all stations over the whole year 2004 for methane (top left), carbon monoxide (top right), hydrogen (bottom left) and methyl-chloroform (MCF, bottom right). Slopes a and correlation coefficients r of linear regressions [mod] = a[obs]+b are also indicated.

Table 3. Total emitted masses (Tg) of CH$_4$, CO and H$_2$ during 2004 for this study. Ocean sources for CO are 17.2 Tg prior and 21.5 Tg optimized; ocean sources for H$_2$ are 4.5 Tg prior and 4.6 Tg optimized. For CH$_4$, comparison with the updated Bousquet et al. (2006). Prior values are in plain font and optimized values in bold.

| | CH$_4$ | | | | CO | | H$_2$ | |
| | Updated Bousquet et al. (2006) | | this study | | this study | | this study | |
Area	prior	**optimization range**	**optimized**	prior	**optimized**	prior	**optimized**	prior
North America	71.3	**59.4–77.5**	**67.7**	67.0	**188.2**	136.5	**5.3**	5.8
South America	84.8	**67.0–94.8**	**67.1**	71.8	**131.3**	146.0	**3.3**	4.7
Europe	71.1	**51.9–64.6**	**56.3**	58.1	**128.0**	102.5	**4.3**	4.6
Africa	63.9	**74.8–95.0**	**64.1**	61.4	**317.1**	264.2	**7.1**	7.5
Boreal Eurasia	29.2	**22.3–28.1**	**28.5**	32.3	**79.3**	24.1	**0.8**	0.8
India + China	121.6	**113.9–149.6**	**162.6**	152.4	**459.4**	272.0	**8.1**	8.5
Australia + Indonesia	40.3	**38.5–54.9**	**44.7**	45.1	**88.1**	96.1	**2.7**	2.9
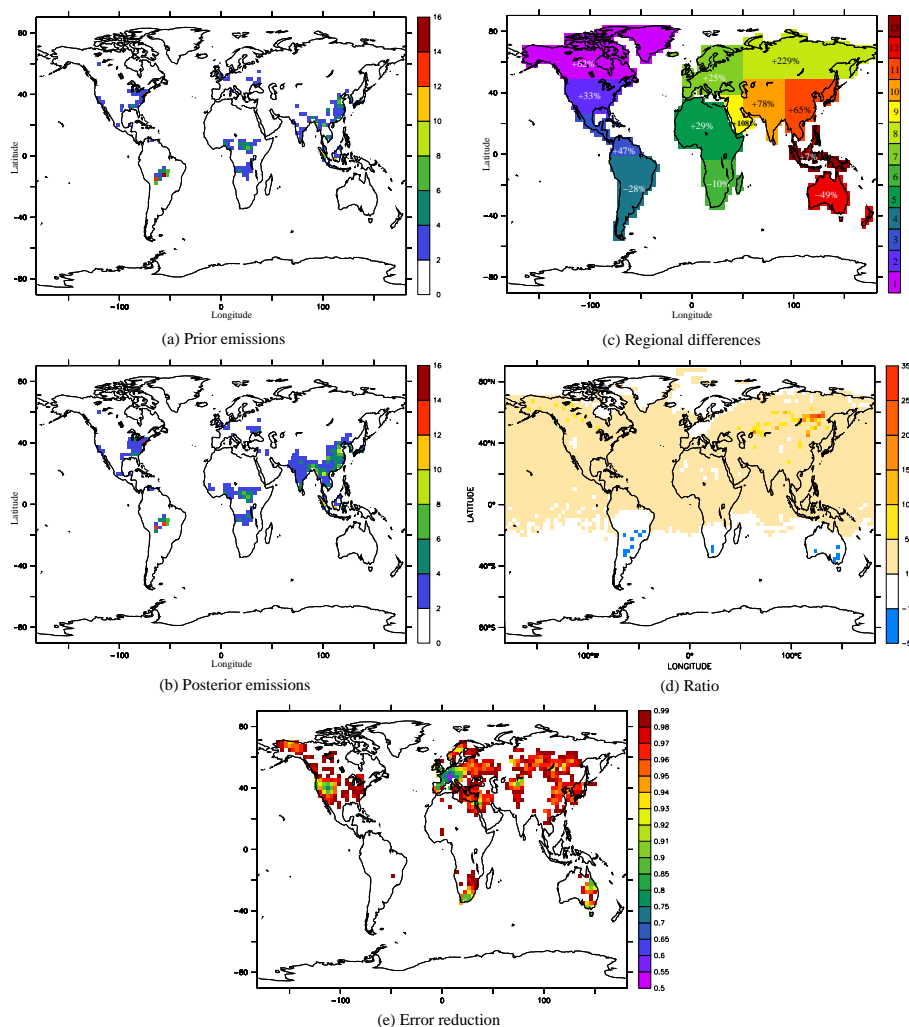
Fig. 5. (a–b): prior (a, top left) and posterior (b, middle left) emitted masses of CO per pixel for the year 2004. (**c**, top right): Difference in % of the prior emission flux between optimized and a priori emission fluxes of CO per region for 2004. 1 = North America boreal, 2 = USA, 3 = America tropical, 4 = South America temperate, 5=Northern Africa, 6 = Southern Africa, 7 = Europe, 8 = Eurasia boreal, 9 = Middle East, 10 = Indian peninsula, 11 = East Asia, 12 = Australia, 13 = Indonesia. (**d**, middle right): Ratio between optimized and a priori CO emission fluxes per pixel for 2004. (**e**, bottom): Error reduction for CO fluxes computed from statistics of 96 realizations per pixel, white areas indicate values higher than 0.99.

is 69 ppbv for the observations and only 51 ppbv for the first-guess. After optimization, the North-South gradient is 70.5 ppbv: the difference with the observations is reduced by almost 92%. Thus, as displayed in Fig. 5c and in Table 3 (note that the regions are not defined in exactly the same way in the figure and in the table), the spatial distribution of corrections is not homogeneous. The emitted mass is decreased in the Southern Hemisphere, in the tropical area of South-America, in Southern Africa and in Australia, whereas it is increased by more than 60% in the boreal areas of North-America and Eurasia and in the developing India and China. As a result, the total emitted mass of CO is increased by more than 30% (Table 2) with regional changes up to 78%

and 65% in East Asia and in the Indian peninsula. This underestimation of CO emissions in Asia has been previously noticed (Carmichael et al., 2003; Palmer et al., 2003; Heald et al., 2004; Pétron et al., 2004). The increase in North America is partly due to boreal Canada and Alaska, two regions concerned by extended fires in 2004, as described by Pfister et al. (2005) and Turquety et al. (2007). For the area defined as "North America boreal" in the TRANSCOM experiment (Gurney et al. (2004), see also www.purdue.edu/transcom), the study by Pfister et al. (2005) gives posterior emissions of CO in summer of 30($\pm$5) Tg from fires and Turquety et al. (2007) give 19 Tg from fires and 11 Tg from peat. Since we do not separate processes in our inversion, this is to be
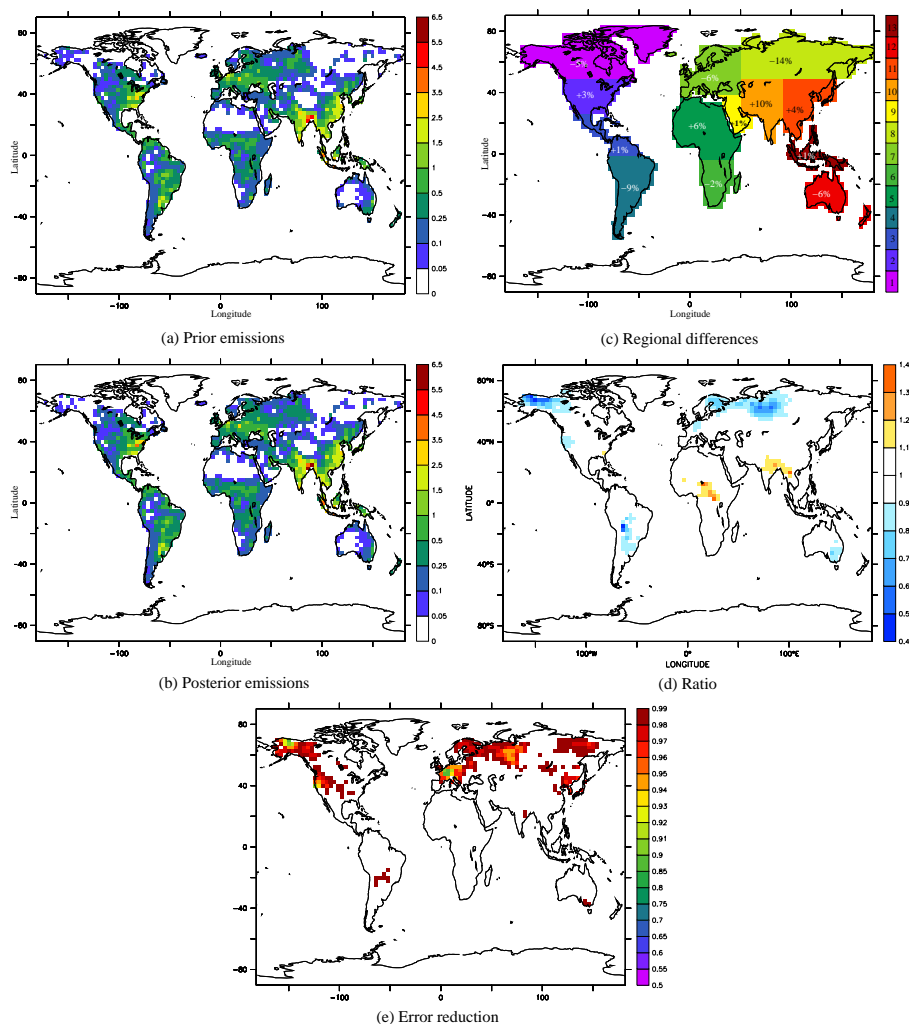
(a) Prior emissions

(c) Regional differences

(b) Posterior emissions

(d) Ratio

(e) Error reduction

Fig. 6. (a–b): prior (a, top left) and posterior (b, middle left) emitted masses of CH$_4$ per pixel for the year 2004. (**c**, top right): Difference in % of the prior emission flux between optimized and a priori emission fluxes of CH$_4$ per region for 2004. 1 = North America boreal, 2 = USA, 3 = America tropical, 4 = South America temperate, 5 = Northern Africa, 6 = Southern Africa, 7 = Europe, 8 = Eurasia boreal, 9 = Middle East, 10 = Indian peninsula, 11 = East Asia, 12 = Australia, 13 = Indonesia. (**d**, middle right): Ratio between optimized and a priori CH$_4$ emission fluxes per pixel for 2004. (**e**, bottom): Error reduction for CH$_4$ fluxes computed from statistics of 96 realizations per pixel, white areas indicate values higher than 0.99.

compared to our posterior of 18.8 Tg in the same area for the same summer. Our results are then in the lower bound of the range of analyzed emissions.

CH$_4$ Even though the total emitted mass of CH$_4$ is modified by only 0.2% (Table 2), changes can reach -14% at the continental scale and +40% at the pixel scale (Table 3 and Fig. 6d, note that the regions are not defined in exactly the same way in the figure and in the table). The spatial distribution of the ratio between optimized and first-guess fluxes in each pixel displayed in Fig. 6d and in Table 3 shows that the inversion redistributes the emissions to a large extent. At a continental scale, emissions are reduced by 14% in Boreal Eurasia and by 6% in Europe and increased by 13% in East Asia (In-

dia + China). At the pixel scale, in the Northern Hemisphere, methane fluxes are increased 1.1 to 1.4 times in three areas in the Tropics (in the center of Africa and in North India and South China) whereas they are decreased 1.1 to 2.5 times at higher latitudes (in Alaska, Scandinavia and the North of Russia).

H$_2$ The decrease by 8% in total H$_2$ emissions is due to particular areas, as displayed in Fig. 7 and quantified at a continental scale in Table 3. Some of these areas correspond to the surroundings of point where constraints are available as in the case of Australia with station CGO or in East China around station TAP. In other areas, such as South America, Africa, Indonesia, China, Europe, USA, the corrections of
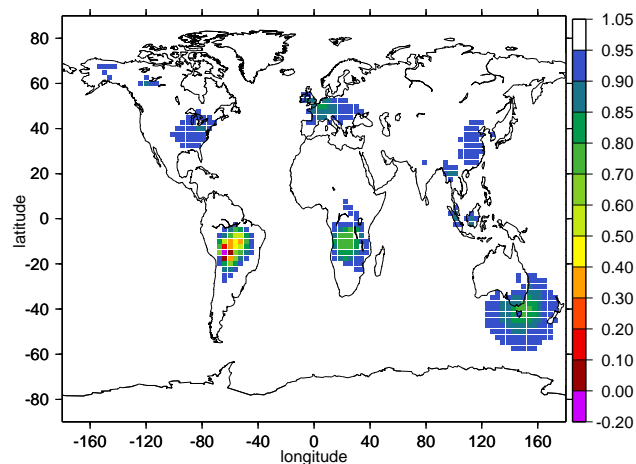
Fig. 7. Ratio between optimized and a priori H$_2$ emission fluxes per pixel for 2004.

Fig. 8. Difference between mono- and multi-species optimized CO emitted masses (in Tg) per pixel for 2004. Positive values indicate the mono-species inversion gives larger emissions than the multi-species inversion.

the fluxes may be large locally: optimized fluxes can be up to 10 times smaller than the prior and their signs can be opposite like in South America for one pixel (Fig. 7). The large corrections seem to be linked to the high deposition velocities prescribed (more than 0.05 cm s^{-1} on average in 2004). The lack of atmospheric constraints in regions like South America can also lead to particularly large flux corrections, with a decrease of 80% at the pixel scale in absolute value and 40% for the whole area (Table 3). The distinction between emission and deposition fluxes in the inversion is technically feasible but would require more constraints, such as isotopic measurements or more precision on the spatio-temporal distribution of the various types of sources and sinks.

Error reduction

The error reduction is computed by the Monte-Carlo approach of Chevallier et al. (2007). Briefly, several inversions are run with observational constraints obtained from "true" concentrations which are actually outputs of a forward simulation, perturbed by a realization of the observation error statistics R. For each inversion, the seed of the random distribution and therefore the set of "measurements" is different. The first-guess fluxes are generated by perturbing the "true" fluxes with a realization of the prior error statistics B (see Sect. 2.1). After inversion, the difference between the "true" fluxes and the analyzed fluxes is computed and compared to the difference between the "true" and the first-guess fluxes. The error reduction is computed as the ratio of the analyzed standard deviation to the first-guess standard deviation of these differences.

The results obtained with a statistical ensemble of 96 fluxes for each pixel are displayed in Figs. 5 and 6. For CO (Fig. 5e), the reduction is larger around the stations, with reductions by more than 10% around PTA (Point Arena, Cal-
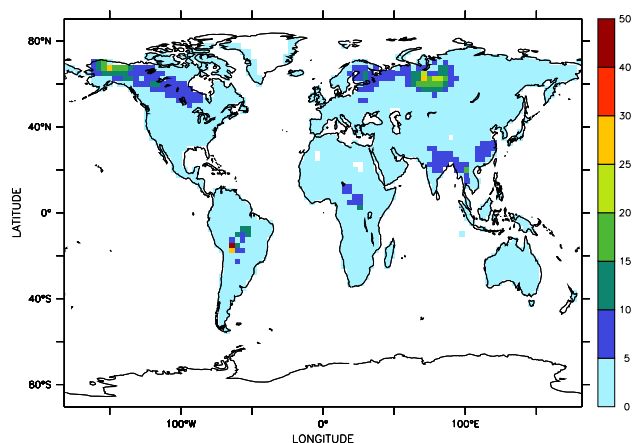
ifornia) and UTA (Wendover, Utah) on the Pacific Coast of the USA, in South Africa around CPT (Cape Point), in Australia at CFA (Cape Ferguson) and reductions up to 50% in Western Europe, where stations are close and numerous. For CH$_4$ (Fig. 6e), error reductions by more than 1% occur only in the Northern Hemisphere: up to 10% in Western Europe and Alaska, more than 5% on the Pacific Coast of the USA. Note that these are theoretical results in the case of a statistically consistent inversion system and assuming very large prior uncertainties. Therefore, the figures for the error reduction are optimistic and only the relative variations are meaningful.

3.3 Sensitivity to multi-species inversion

In order to assess the advantage of running a multi-species inversion instead of a mono-species one, two mono-species inversions are run. In these inversions, only the emission fluxes of either CO or CH$_4$ are optimized with either CO or CH$_4$ observations as constraints (the state vector therefore does not include OH concentrations).

In the CO mono-species inversion, CO emissions are increased by 34.9% instead of 33.5% for the multi-species case, the chemical loss of CO is increased by 15% instead of 12.9% and the chemical production of CO is only changed by 0.03% (instead of 2.7%) together with the chemical loss of CH$_4$ which is increased by 0.06%. All the other balances are left unchanged as compared to the prior. The results obtained after the mono-species inversion are close to the results obtained for CO in the multi-species system. But the differences are that i) the median bias at the stations is −1.0 ppbv after the mono-species inversion versus −0.6 ppbv after the multi-species inversion and ii) the
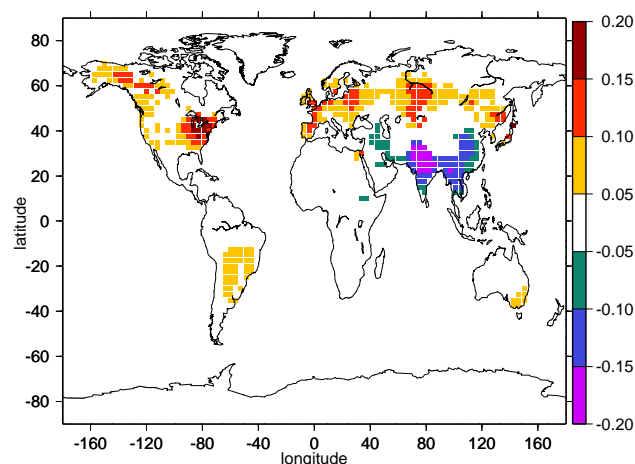
Fig. 9. Difference between mono- and multi-species optimized CH$_4$ emission fluxes (in % of the multi-species optimized fluxes) per pixel for 2004. Positive values indicate the mono-species inversion gives larger emissions than the multi-species inversion.

differences between optimized fluxes are significant in particular regions. The differences between optimized masses obtained with the mono- and multi-species inversions are displayed in Fig. 8 at a pixel scale. The mono-species inversion leads to larger emitted masses than the multi-species case in regions North America boreal (+23 percentage points), USA (+6 percentage points), Europe (+6 percentage points) and Eurasia boreal (+33 percentage points). In the region of the Indian peninsula, the mono-species emitted masses are lower (−6 percentage points) than the multi-species results.

After the CH$_4$ mono-species inversion, CH$_4$ emissions are increased by 3.4% to 506.9 Tg versus +0.2% for the multi-species case and the chemical production of CO is increased by 0.07%. All the other balances are left unchanged as compared to the prior. The median bias after the mono-species inversion is (−0.5 ppbv versus (−0.1 ppbv for the multi-species inversion. The difference between optimized fluxes obtained with the mono- and multi-species inversions are displayed in Fig. 9 at a pixel scale: the mono-species analyzed fluxes are higher by up to 50% than the multi-species analyzed fluxes. The increase from the prior fluxes in the three tropical areas (center of Africa, North India and South China) are higher by up to 11 % than with the multi-species inversion (Fig. 6d) whereas the decrease at higher latitudes (Alaska, Scandinavia, North Russia) is lower by up to 30%. These results can be explained by the fact that OH concentrations are not modified by the mono-species inversion whereas the multi-species inversion lowered them globally. Therefore, to fit the same constraints in CH$_4$ concentrations with higher OH concentrations i.e. with a higher chemical loss of CH$_4$, the mono-species inversion only has the possibility of increasing the emission fluxes.

The multi-species approach takes into account the complexity of the interactions between species so that consistent results are obtained in one inversion for a number of tracers. The results obtained with the multi-species system are not globally different from the results of a mono-species inversion for CO; for CH$_4$, the difference between the two methods amounts to less than 50% of the inter-annual variability ($\approx$10% in mass in Bousquet et al. (2006)). At a regional scale, the results may show significant differences as compared to the mono-species inversions: coupling CO with other species significantly changes the regional distribution of analyzed CO emissions.

3.4 Comparison with other data

We compare the results of our multi-species inversion to results obtained in another study inverting one of the species of interest and to observation data (satellite, aircraft and ship data) that have not been used in our inversions. These comparisons are a first attempt at evaluating our optimized fluxes. Note that as most fixed surface data are used in the inversion, we do not have independent fixed surface stations to compare our results with in 2004.

Other inversion system For CH$_4$, Bousquet et al. (2006) computed a range of emissions from 1984 to 2003. This study has been updated to 2004, using the same prior emissions, inverse system and assumptions but updated MCF and CH$_4$ observations. The results for 2004 are compared in Table 3 to our results in seven areas. For four regions (North and South Americas, Europe, South Asia), our estimate is within the range of Bousquet's results; for two other regions (Boreal Eurasia and India+China) our emissions are above the maximum of Bousquet's range by 8.4 and 3.1% respectively; in Africa, our result is under the minimum by 13%. Comparing the results for the tropical regions indicates a shift of emissions from South America and Africa for the study of Bousquet et al. (2006) to India + China in our study. This difference in attributing methane emissions in the Tropics may be due to the cumulative effects of aggregation errors for the study of Bousquet et al. (2006) and to the small number of available stations in this area for both studies. Our CH$_4$ optimized emissions seem to be statistically consistent with the results of a completely different system.

Mobile surface and aircraft CH$_4$ measurements For the year 2004, 456 mobile surface observations of CH$_4$ concentrations are available through the Pacific Ocean, Atlantic Ocean and Western Pacific Cruises (POC, AOC, WPC) (Conway et al., 1994), ships in the North Atlantic (CVS) and in the Indian Ocean (MDF, Marion Dufresne ship) (RAMCES network (Schmidt et al., 2006)) and 202 three-dimensional observations are given by aircraft measurements made in Hungary (HNG, 12 flights in the year, none in February and March, 2 in April and December, 1 for the other months) and in France (ORL, 25 flights in the year, 1 in January, March and April, 2 in June and August, none in December, 3 for

Table 4. Slope a and correlation coefficient r of linear regressions of simulated against observed CH$_4$ and CO concentrations for different observation types. Bias and standard deviation between simulated and observed concentrations for the same samples. NO = number of observations. std dev. = standard deviation. BL = Boundary Layer, up to ≈1100 m in the model. NH = Northern Hemisphere, SH = Southern Hemisphere.

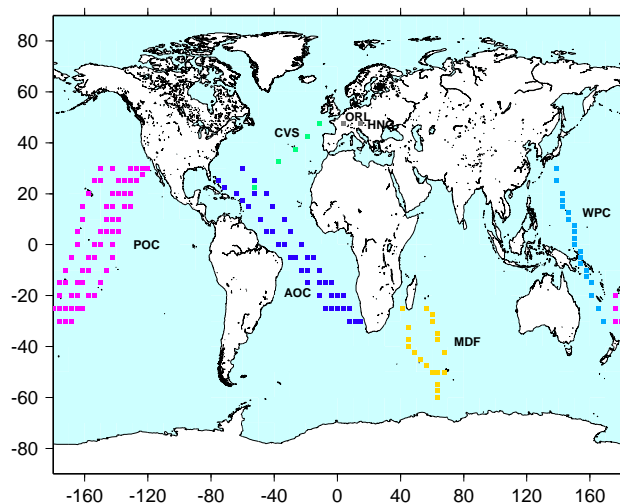| Species	Type of measurements		a	r	bias (ppbv)	std dev. (ppbv)
CH$_4$	ocean data	First-guess	0.97	0.96	−−2.1	11.5
	NO = 456	Analysis	0.98	0.96	−1.8	10.9
	aircraft data (BL)	First-guess	1.04	0.73	−1.7	28.0
	NO = 113	Analysis	0.86	0.7	−4.3	21.2
CO	MOPITT NH	First-guess	0.63	0.57	−12.7	19.2
	NO ≈ 436 500	Analysis	0.78	0.58	14.2	25.8
	MOPITT SH	First-guess	0.85	0.77	−9.8	15.8
	NO ≈ 441 500	Analysis	0.95	0.78	−8.4	18.0

Fig. 10. Locations of the ocean and aircraft measurements of CH$_4$ concentrations for 2004. Colors for ships: pink = POC, blue = AOC, green = CVS, yellow = MDF, light blue = WPC; grey = aircraft sites.
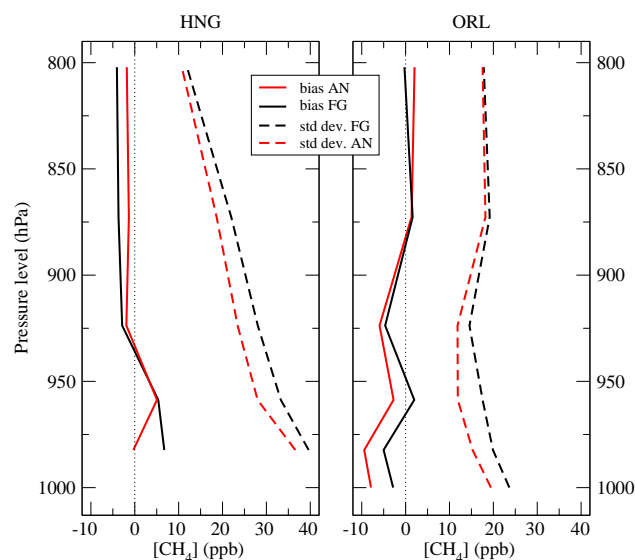

Fig. 11. Vertical profiles of bias (solid lines) and standard deviation (std dev., dashed lines) between measured and first-guess (FG, in black) or analyzed (AN, in red) CH$_4$ concentrations (ppbv) at ORL and HNG locations in 2004. Positive values for the bias indicate that the simulated concentrations are higher than the measurements.

the other months) (Schmidt et al., 2006) (locations displayed in Fig. 10). These data were compared to simulated concentrations before and after inversion through scatter-plots (not shown): the results of the regressions of simulated concentrations as functions of observations are displayed in Table 4. The fit between simulation and ocean surface data, which is already quite good as a first-guess, is not significantly changed by the inversion (the slope is increased from 0.97 to 0.98 for the same correlation coefficient). Since these measurements are made in the oceans, far from the sources, this shows that simulated background concentrations are as good with the analysis as with the prior.

The aircraft data in the boundary layer (113 measurements) show a bias between model and observations of −1.7 ppbv before inversion (Table 4) and −4.3 ppbv after the optimization of emissions. The vertical profiles of bias and standard

deviation between measurements and the first-guess or analyzed simulated CH$_4$ concentrations are displayed in Fig. 11. They show that the inversion has a positive impact on the bias near the surface at HNG, as expected, but a negative impact at ORL. The inversion has a positive impact on the standard deviation at both places: the standard deviation is reduced by 7.5 to 16.5% at HNG and 1.5 to 32% at ORL. The two sites are very different: ORL is under rather marine influence most of the time whereas HNG is a continental site i.e. under the influence of industrial and natural sources. It is known that the forward models are less accurate in continental sites than in "oceanic" ones because of the influence of the multiple

types of sources that is to be taken into account (Geels et al., 2007).

Satellite data MOPITT CO measurements are available for 2004 (Emmons et al., 2007). We use here retrievals at 700 hPa of concentration product (level 2 version 5) with individual averaging kernels (Deeter et al., 2003, 2004; Emmons et al., 2004; Edwards et al., 1999) sampled to keep only daytime measurements as described by Chevallier et al. (2009). Since the quality of the satellite data is not the same over ocean and continents, the data are compared to simulated concentrations before and after inversion through scatter-plots for the Northern and the Southern Hemispheres separately: the results of the regressions of simulated concentrations as functions of observations are displayed in Table 4. The inversion increases by 24 and 12% the slopes in the Northern and Southern Hemispheres respectively. Nevertheless, the comparison with MOPITT shows an underestimation by ≈22% of analyzed CO concentrations in the Northern Hemisphere that could be due to difficulties to reproduce the high emissions due to the fires that occurred in 2004 in Alaska and Canada boreal areas (see paragraph "Emissions" in Sect. 3.2).

4 Conclusions

We have developed a variational system based on the LMDz transport model and on a simplified chemistry system, SACS, representing the oxidation chain of methane, to perform multi-species inversions of CH₄, CO and H₂ surface emissions at model resolution and for the year 2004. OH concentrations are optimized simultaneously, as constrained by methyl-chloroform atmospheric observations.

Results show significant modifications in the total emitted masses and in the spatial distribution of the emissions as compared to the prior. For CO, the total emitted mass is increased by 30%. A large increase by more than 65% in the regions of East Asia and the Indian peninsula corrects for the known underestimation of CO emissions in these rapidly developing areas (increased emissions by industry, traffic and population). A particular feature of the year 2004 is captured in boreal North America: the increase by more than 60% of CO emissions in Alaska and Canada may be related to the intense fires that occurred this year. For almost the same total emissions, the spatial distribution of CH₄ fluxes is significantly modified with increased fluxes in the Tropics (+10 to +40% in Africa, India and China) and decreased fluxes in boreal areas (−10 to −60% in Alaska, Scandinavia and Russia). Estimated error reductions for analyzed emissions (at the spatial resolution of the grid cell and for an eight-day time resolution) are larger in Western Europe (50% for CO and 10% for CH₄) because of the higher density of the measurement networks in this area.

Even though the global balances obtained with the multi-species system are not very different from the results of a mono-species inversion at the global scale, regional differences are significant, particularly for CH₄ (in North America, Europe, boreal Eurasia and India). In practice, the analyzed fluxes of all the tracers are obtained in one consistent inversion.

The comparison of our analyzed fluxes with the results obtained by another inversion system by Bousquet et al. (2006) shows that they lie in the same range. The comparison of our analyzed CH₄ concentrations with independent measurements by mobile surface stations and aircraft shows no significant improvement for the background conditions (over the oceans) and a significant improvement in the vertical profile of standard deviation in the boundary layer and in the free troposphere. The comparison of CO concentrations to independent satellite data shows that the fit between simulation and measurements is significantly better in both hemispheres after the inversion, which indicates that the inverse system is able to correct for large underestimations in the prior and obtain consistent analyzed fluxes.

This work shows the promising perspectives of such a multi-species inversion system both to provide better emission fluxes and to exploit in synergy various types of observations. The next step is now to use satellite observations, such as SCIAMACHY CH₄ columns and MOPITT CO columns, and surface measurements simultaneously as constraints in a multi-species inversion.

Edited by: W. Lahoz

References

Bergamaschi, P., Frankenberg, F., Meirink, J. F., Krol, M., Dentener, F., Wagner, T., Platt, U., Kaplan, J. O., Körner, S., Heimann, M., Dlugokencky, E. J., and Goede, A.: Satellite chartography of atmospheric methane from SCIAMACHY on board ENVISAT: 2. Evaluation based on inverse model simulations, J. Geophys. Res., 112, doi:10.1029/2006JD007268, 2007.

Boucher, O., Moulin, C., Belviso, S., Aumont, O., Bopp, L., Cosme, E., von Kuhlmann, R., Lawrence, M. G., Pham, M., Reddy, M. S., Sciare, J., and Venkataraman, C.: DMS atmospheric concentrations and sulphate aerosol indirect radiative forcing: a sensitivity study to the DMS source representation and oxidation, Atmos. Chem. Phys., 3, 49–65, 2003,
http://www.atmos-chem-phys.net/3/49/2003/.

Bousquet, P., Peylin, P., Ciais, P., Le Quere, C., Friedlingstein, P., and Tans, P.: Regional changes in carbon dioxide fluxes of land and ocean since 1980., Science, 290, 1342–1345, 2000.

Bousquet, P., Hauglustaine, D., Peylin, P., Carouge, C., and Ciais, P.: Two decades of OH variability as inferred by an inversion of atmospheric transport and chemistry of methyl chloroform, Atmos. Chem. Phys., 5, 2635–2656, 2005.

Bousquet, P., Ciais, P., Miller, J. B., Dlugokencky, E. J., Hauglustaine, D. A., Prigent, C., Van der Werf, G. R., Peylin, P., Brunke, E. G., Carouge, C., Langenfelds, R. L., Lathiere, J., Papa, F., Ramonet, M., Schmidt, M., Steele, L. P., Tyler, S. C., and White, J.: Contribution of anthropogenic and natural sources to atmospheric methane variability, Nature, 443, 439–443, doi: {10.1038/nature05132}, 2006.

Butler, T. M., Rayner, P. J., Simmonds, I., and Lawrence, M. G.: Simultaneous mass balance inverse modeling of methane and carbon monoxide, J. Geophys. Res., 110, D21310, doi:10.1029/2005JD006071, 2005.

Carmichael, G., Tang, Y., Kurata, G., Uno, I., Streets, D., Thongboonchoo, N., Woo, J., Guttikunda, S., White, A., Wang, T., et al.: Evaluating regional emission estimates using the TRACE-P observations, J. Geophys. Res., 108(D21), 8823, doi:10.1029/2002JD003117

Carouge, C., Bousquet, P., Peylin, P., Rayner, P., and Ciais, P.: What can we learn from European continuous atmospheric CO_2 measurements to quantify regional fluxes, Part 1: Potential of the network, Atmos. Chem. Phys. Discuss., 8, 18591–18620, 2008a.

Carouge, C., Peylin, P., Rayner, P. J., Bousquet, P., Chevallier, F., and Ciais, P.: What can we learn from European continuous atmospheric CO_2 measurements to quantify regional fluxes, Part 2: Sensitivity of flux accuracy to inverse setup, Atmos. Chem. Phys. Discuss., 8, 18621–18649, 2008b.

Chevallier, F., Fisher, M., Peylin, P., Serrar, S., Bousquet, P., Bréon, F.-M., Chédin, A., and Ciais, P.: Inferring CO_2 sources and sinks from satellite observations: method and application to TOVS data, J. Geophys. Res., 110, L23801, doi:10.1029/2005JD006390, 2005.

Chevallier, F., Bréon, F.-M., and Rayner, P.: The contribution of the Orbiting Carbon Observatory to the estimation of CO_2 sources and sinks: Theoretical study in a variational data assimilation framework, J. Geophys. Res., 112, D09307, doi:10.1029/2006JD007375, 2007.

Chevallier, F., Fortems, A., Bousquet, P., Pison, I., Szopa, S., Devaux, M., and Hauglustaine, D.: African CO emissions between years 2000 and 2006 as estimated from MOPITT observations, Biogeosciences, 6, 103–111, 2009,
http://www.biogeosciences.net/6/103/2009/.

Conway, T. J., Tans, P. P., Waterman, L. S., Thoning, K. W., Kitzis, D. R., Masarie, K. A., and Zhang, N.: Evidence for interannual variability of the carbon cycle from the National Oceanic and Atmospheric Administration/Climate Monitoring and Diagnostic Laboratory Global Air Sampling Network, J. Geophys. Res., 99, 22831–22855, 1994.

Cunnold, D., Steele, L., Fraser, P., Simmonds, P., Prinn, R., Weiss, R., Porter, L., O'Doherty, S., Langenfelds, R., Krummel, P., et al.: In situ measurements of atmospheric methane at GAGE/AGAGE sites during 1985–2000 and resulting source inferences, J. Geophys. Res., 107, 4225, 2002.

Deeter, M., Emmons, L., Francis, G., Edwards, D., Gille, J., Warner, J., Khattatov, B., Ziskin, D., Lamarque, J.-F., Ho, S.-P., Yudin, V., Attié, J.-L., Packman, D., Chen, J., Mao, D., and Drummond, J.: Operational carbon monoxide retrieval algorithm and selected results for the MOPITT instrument, J. Geophys. Res., 108(D14), 4399, doi:10.1029/2002JD003186, 2003.

Deeter, M., Emmons, L., Edwards, D., Gille, J., and Drummond, J.: Vertical resolution and information content of CO profiles retrieved by MOPITT, Geophys. Res. Lett., 31, L15112, doi:10.1029/2004GL020235, 2004.

Dlugokencky, E., Steele, L., Lang, P., and Masarie, K.: The growth rate and distribution of atmospheric methane, J. Geophys. Res., 99, 1994.

Dlugokencky, E., Myers, R., Lang, P., Masarie, K., Crotwell, A., Thoning, K., Hall, B., Elkins, J., and Steele, L.: Conversion of NOAA atmospheric dry air CH_4 mole fractions to a gravimetrically prepared standard scale, J. Geophys. Res, 110, D18306, doi:10.1029/2005JD006035, 2005.

Dubovik, O., Lapyonok, T., Kaufman, Y., Chin, M., Ginoux, P., Kahn, R., and Sinyuk, A.: Retrieving global aerosol sources from satellites using inverse modeling, Atmos. Chem. Phys., 8, 209–250, 2008, http://www.atmos-chem-phys.net/8/209/2008/.

Edwards, D., Halvorson, C., and Gille, J.: Radiative transfer modeling of the EOS Terra Satellite MOPITT instrument, J.Geophys. Res., 104(D14), 16755–16775, doi:10.1029/2002JD002378, 1999.

Elbern, H., Strunk, A., Schmidt, H., and Talagrand, O.: Emission rate and chemical state estimation by 4-dimensional variational inversion, Atmos. Chem. Phys., 7, 3749–3769, 2007,
http://www.atmos-chem-phys.net/7/3749/2007/.

Emmons, L., Deeter, M., Gille, J., Edwards, D., and Attie, J.-L.: Validation of measurements of MOPITT CO retrievals with aircraft in situ profiles, J. Geophys. Res., 108, D03309, doi:10.1029/2003JD004101, 2004.

Emmons, L., Pfister, G., Edwards, D., Gille, J., Sachse, G., Blake, D., Wofsy, S., Gerbig, C. ans Matross, D., and Nedelec, P.: MOPITT validation exercises during summer 2004 field campaigns over North America, J. Geophys. Res., 112, D12S02, doi:10.1029/2006JD007833, 2007.

Folberth, G., Hauglustaine, D., Ciais, P., and Lathière, J.: On the role of atmospheric chemistry in the global CO_2 budget, Geophys. Res. Lett., 32, L08801, doi:10.1029/2004GL021812, 2005.

Folberth, G. A., Hauglustaine, D. A., Lathière, J., and Brocheton, F.: Interactive chemistry in the Laboratoire de Météorologie Dynamique general circulation model: model description and impact analysis of biogenic hydrocarbons on tropospheric chem-

istry, Atmos. Chem. Phys., 6, 2273–2319, 2006,
http://www.atmos-chem-phys.net/6/2273/2006/.

Francey, R., Steele, L., Langenfelds, R., and Pak, B.: High Precision Long-Term Monitoring of Radiatively Active and Related Trace Gases at Surface Sites and from Aircraft in the Southern Hemisphere Atmosphere, J. Atmos. Sci., 56, 279–285, 1999.

Frankenberg, C., Meirink, J., van Weele, M., Platt, U., and Wagner, T.: Assessing methane emissions from global space-borne observations, Science, 308, 1010–1014, doi:{10.1126/science. 1106644}, 2005.

Fung, I., John, J., Lerner, J., Matthews, E., Prather, M., Steele, L., and Fraser, P.: Three-dimensional model synthesis of the global methane cycle, J. Geophys. Res., 96, 13033–13065, 1991.

Geels, C., Gloor, M., Ciais, P., Bousquet, P., Peylin, P., Vermeulen, A., Dargaville, R., Aalto, T., Brandt, J., Christensen, J., et al.: Comparing atmospheric transport models for future regional inversions over Europe–Part˜ 1: mapping the atmospheric CO_2 signals, Atmos. Chem. Phys., 7, 3461–3479, 2007, http://www.atmos-chem-phys.net/7/3461/2007/.

Gilbert, J.-C. and Lemaréchal, C.: Some numerical experiments with variable-storage quasi-Newton algorithms, Math. Program., 45, 407–435, 1989.

GLOBALVIEW-CH4: Cooperative Atmospheric Data Integration Project - Methane, NOAA ESRL (Boulder, Colorado), CD-ROM [Also available on Internet via anonymous FTP to ftp.cmdl.noaa. gov, Path: ccg/ch4/GLOBALVIEW], 2005.

GLOBALVIEW-CO: Cooperative Atmospheric Data Integration Project - Carbon Monoxide, NOAA ESRL (Boulder, Colorado), CD-ROM [Also available on Internet via anonymous FTP to ftp.cmdl.noaa.gov, Path: ccg/co/GLOBALVIEW], 2005.

Gurney, K., Law, R., Denning, A., Rayner, P., Pak, B., Baker, D., Bousquet, P., Bruhwiler, L., Chen, Y., Ciais, P., et al.: Transcom 3 inversion intercomparison: Model mean results for the estimation of seasonal carbon sources and sinks, Global Biogeochem. Cy., 18, GB1010, doi:10.1029/2003GB002111, 2004.

Gurney, K., Law, R., Denning, A., Rayner, P., Baker, D., Bousquet, P., Bruhwiler, L., Chen, Y., Ciais, P., Fan, S., Fung, I., Gloor, M., Heimann, M., Higuchi, K., John, J., Maki, T., Maksyutov, S., Masarie, K., Peylin, P., Prather, M., Pak, B., Randerson, J., Sarmiento, J., Taguchi, S., Takahashi, T., and Yuen, C.: Towards robust regional estimates of CO_2 sources and sinks using atmospheric transport models, Nature, 415, 626–630, 2002.

Hauglustaine, D. and Ehhalt, D.: A three-dimensional model of molecular hydrogen in the troposphere, J. Geophys. Res., 107(D17), 4330, doi:{10.1029/2001JD001156}, 2002.

Hauglustaine, D., Hourdin, F., Jourdain, L., Filiberti, M., Walters, S., Lamarque, J., and Holland, E.: Interactive chemistry in the Laboratoire de Météorologie Dynamique general circulation model: Description and background tropospheric chemistry evaluation, J. Geophys. Res., 109, D04314, doi:10.1029/ 2003JD003957, 2004.

Heald, C., Jacob, D., Jones, D., Palmer, P., Logan, J., Streets, D., Sachse, G., Gille, J., Hoffman, R., and Nehrkorn, T.: Comparative inverse analysis of satellite (MOPITT) and aircraft (TRACE-P) observations to estimate Asian sources of carbon monoxide, J. Geophys. Res, 109, D23306, doi:10.1029/2004JD005185, 2004.

Hourdin, F. and Armengaud, A.: The use of finite-volume methods for atmospheric advection of trace species. Part I: Test of various formulations in a general circulation model, Mon. Weather Rev.,

127, 822–837, 1999.

IPCC: Climate change 2007 – Synthesis Report, Cambridge University Press, 996 pp., 2007.

Krol, M., Lelieveld, J., Oram, D., Sturrock, G., Penkett, S., Brenninkmeijer, C., Gros, V., Williams, J., and Scheeren, H.: Continuing emissions of methyl chloroform from Europe, Nature, 421, 131–135, doi:{10.1038/nature01311}, 2003.

Lowe, D., Brenninkmeijer, C., Tyler, S., and Dlugkencky, E.: Determination of the Isotopic Composition of Atmospheric Methane and its Application in the Antarctic, J. Geophys. Res., 96, 15455–15467, 1991.

Matsueda, H., Sawa, Y., Wada, A., Inoue, H. Y., Suda, K., Hirano, Y., Tsuboi, K., and Nishioka, S.: Methane standard gases for atmospheric measurements at the MRI and JMA and intercomparison experiments, Pap. Meteor. Geophys., 54, 91–109, 2004.

Meirink, J. F., Bergamaschi, P., and Krol, M. C.: Four-dimensional variational data assimilation for inverse modelling of atmospheric methane emissions: method and comparison with synthesis inversion, Atmos. Chem. Phys., 8, 6341–6353, 2008, http://www.atmos-chem-phys.net/8/6341/2008/.

Montzka, S., Spivakovsky, C., Butler, J., Elkins, J., Lock, L., and Mondeel, D.: New Observational Constraints for Atmospheric Hydroxyl on Global and Hemispheric Scales, Science, 288, 500, 2000.

Novelli, P., Steele, P., and Tans, P.: Mixing ratios of carbon monoxide in the troposphere, J. Geophys. Res., 97(D18), 20731–20750, 1992.

Novelli, P., Lang, P., Masarie, K., Hurst, D., Myers, R., and Elkins, J.: Molecular hydrogen in the troposphere- Global distribution and budget, J. Geophys. Res., 104(D23), 30427–30444, 1999.

Ohara, T., Akimoto, H., Kurokawa, J., Horii, N., Yamaji, K., Yan, X., and Hayasaka, T.: An Asian emission inventory of anthropogenic emission sources for the period 1980–2020, Atmos. Chem. Phys., 7, 4419–4444, 2007, http://www.atmos-chem-phys.net/7/4419/2007/.

Olivier, J. G. J. and Berdowski, J. J. M.: The Climate System, chap. Global emissions sources and sinks, A. A. Balkema/Swets & Zeitlinger, J. Berdowski, R. Guichert, B. Heij, 33–37, 2001.

Palmer, P., Jacob, D., Jones, D., Heald, C., Yantosca, R., Logan, J., Sachse, G., and Streets, D.: Inverting for emissions of carbon monoxide from Asia using aircraft observations over the western Pacific, J. Geophys. Res., 108(D21), 8828, doi:10.1029/2003JD003397, 2003.

Pétron, G., Granier, C., Khattatov, B., Yudin, V., Lamarque, J., Emmons, L., Gille, J., and Edwards, D.: Monthly CO surface sources inventory based on the 2000-2001 MOPITT satellite data, Geophys. Res. Lett., 31, L21107.1–L21107.5, doi: {10.1029/2004GL020560}, 2004.

Peylin, P., Rayner, P. J., Bousquet, P., Carouge, C., Hourdin, F., Heinrich, P., Ciais, P., and contributors, A.: Daily CO_2 flux estimates over Europe from continuous atmospheric measurements: 1, inverse methodology, Atmos. Chem. Phys., 5, 3173–3186, 2005, http://www.atmos-chem-phys.net/5/3173/2005/.

Pfister, G., Hess, P., Emmons, L., Lamarque, J.-F., Wiedinmyer, C., Edwards, D., Pétron, G., Gille, J., and Sachse, G.: Quantifying CO emissions from the 2004 Alaskan wildfires using MOPITT CO data, Geophys. Res. Lett., 32, L11809, doi:10.1029/2005GL022995, 2005.

Price, H., Jaeglé, L., Rice, A., Quay, P., Novelli, P. C., and

Gammon, R.: Global budget of molecular hydrogen and its deuterium content: Constraints from ground station, cruise, and aircraft observations, J. Geophys. Res., 112, D22108, doi:10.1029/2006JD008152, 2007.

Prinn, R., Huang, J., Weiss, R., Salameh, P., Miller, B., Fraser, P., Simmonds, P., O'Doherty, S., Cunnold, D., and Alyea, F.: A history of chemically and radiatively important gases in air deduced from ALE/GAGE/AGAGE, J. Geophys. Res., 105(D14), 17751–17792, 2000.

Prinn, R., Huang, J., Weiss, R., Cunnold, D., Fraser, P., Simmonds, P., McCulloch, A., Harth, C., Reimann, S., Salameh, P., O'Doherty, S., Wang, R., Porter, L., Miller, B., and Krummel, P.: Evidence for variability of atmospheric hydroxyl radicals over the past quarter century, Geophys. Res. Lett., 32, L07809, doi:10.1029/2004GL022228, 2005.

Rayner, P. J., Enting, I. G., Francey, R. J., and Langenfelds, R.: Reconstructing the recent carbon cycle from atmospheric CO_2, $\delta^{13}C$ and O_2/N_2 observations, Tellus B, 51, 213–232, 1999.

Sadourny, R. and Laval, K.: New Perspectives in Climate Modeling, chap. January and July performance of the LMD general circulation model, edited by: Bergerand, A. L. and Nicolis, C., Amsterdam, The Netherlands, Elsevier press edn., 173–197, 1984.

Schmidt, M., Ramonet, M., Wastine, B., Delmotte, M., Galdemard, P., Kazan, V., Messager, C., Royer, A., Valant, C., Xueref, I., and Ciais, P.: RAMCES: The French Network of Atmospheric Greenhouse Gas Monitoring, in: 13th WMO/IAEA Meeting of Experts on Carbon Dioxide Concentration and Related Tracers Measurement Techniques, Report WMO 168, 165–174, 2006.

Stavrakou, T. and Müller, J.-F.: Grid-based versus big region approach for inverting CO emissions using MOPITT data, J. Geophys. Res., 34, D15304, doi:10.1029/2007GL030231, 2006.

Turquety, S., Logan, J. A., Jacob, D. J., Hudman, R. C., Leung, F. Y., Heald, C. L., Yantosca, R. M., Wu, S., Emmons, L. K., Edwards, D. P., and Sachse, G. W.: Inventory of boreal fire emissions for North America in 2004: Importance of peat burning and pyroconvective injection, J. Geophys. Res., 112, D12S03, doi:{10.1029/2006JD007281}, 2007.

van der Werf, G. R., Randerson, J. T., Giglio, L., Collatz, G. J., Kasibhatla, P. S., and Arellano, Jr., A. F.: Interannual variability in global biomass burning emissions from 1997 to 2004, Atmos. Chem. Phys., 6, 3423–3441, 2006.

Worthy, D., Levin, I., Trivett, N., Kuhlmann, A., Hopper, J., and Ernst, M.: Seven years of continuous methane observations at a remote boreal site in Ontario, Canada, J. Geophys. Res., 103(D13), 15995–16007, 1998.